wrapping a gold wire around the silicon tube about 50 mm from the electrode tip. Electrode impedances were below 6 kiloohms at 1 kHz. Impedances were regularly checked to ensure proper function.
10. Additional control data were published in (*7*) and by J. Popelar, R. Hartmann, J. Syka, and R. Klinke [*Hear. Res.* **92**, 63 (1995)]. Acute deafening of normal hearing cats was performed by intracochlear application of neomycin. Compare also M. W. Raggio and C. E. Schreiner, *J. Neurophysiol.* **72**, 2334 (1994); C. E. Schreiner and M. W. Raggio, *ibid.* **75**, 1283 (1996).
11. E. S. Hochmair, I. J. Hochmair-Desoyer, K. Burian, *Int. J. Artif. Organs* **2**, 255 (1979). The microphone signal was preamplified with automatic gain control (AGC). AGC onset, gain, and output current could be adjusted separately. The frequency response of the current source was adjusted from 0.1 to 6 kHz to produce increasing currents with increasing frequencies according to the decreasing single-fiber sensitivity to higher frequencies under electrical stimulation (*24*). The processor was adjusted to the individual cats by testing their pinna reflex thresholds to gated electrical sinusoids with 0.125 to 8 kHz. The presence of reflexes was judged by observers and monitored by video. Stimulation electrode was selected according to minimal reflex threshold; threshold currents were on the order of 10 μA, set to correspond to 60-dB SPL at 1 kHz.
12. A. Kral, R. Hartmann, D. Mortazavi, R. Klinke, *Hear. Res.* **121**, 11 (1998).
13. Experimental cats were conditioned to receive food pellets upon presentation of a 437-Hz tone burst while the cat stayed in a neutral zone. The cat then had to walk to a food dispenser where a pellet was available for a 5-s time window. Getting food was defined as successful trial.
14. Animals were preanesthetized with ketaminehydrochloride and Combelen (4.5 mg and 2.1 mg/kg body weight, respectively). After tracheotomy, a light isoflurane (0.4 to 0.8%), N_2O (50%), and O_2 anesthesia was maintained [A. Kral, J. Tillein, R. Hartmann, R. Klinke, *Neuroreport* **10**, 781 (1999)]. The skull over the auditory cortex was opened, and the dura was removed. For precise reconstruction of recording positions and tracks, the surface of the cortex was photographed with a digital camera. The dorsal end of the posterior ectosylvian sulcus was used as reference point at 0.0 (Fig. 2). Recording electrodes were positioned by micromotors, with a precision of 1 μm. Electrically evoked field potentials were first recorded by ball silver electrodes, diameter 1 mm. Threshold currents were determined for pulsatile stimuli (charge-balanced, 200 μs per phase, repetition rate = 2.1 per second). Current levels were then raised by 10 dB, a value at which intensity functions start to saturate (about 400 μA peak-to-peak in most cats). The cortex was then scanned (70 to 100 points) with glass microelectrodes (impedance < 10 megaohms). Field potentials were first taken from the surface. Subsequently, depth profiles were taken (300-μm steps). The microelectrodes were also used for recording single-unit and multiunit activity after changing filter settings. Quantitative evaluation for statistical analysis was performed with potentials recorded within a region 1.5 mm by 1.0 mm around the maximal response ("hot spot"). Sample tracks were marked by iontophoretic application of HRP. Determination of layers II, III, and IV was thus reliably achieved. Because of variations in width and angle of penetration set by the location of the hot spot, layers V and VI could not be exactly differentiated. Depth profiles were also used for CSD analyses [see U. Mitzdorf, *Physiol. Rev.* **65**, 37 (1985)].
15. The stimulation was 437 Hz, with a 5-ms duration.
16. Biphasic charge-balanced pulses of 200 μs per phase, with a rate of 2.1 per second and intensity of 10 dB above field potential threshold of the most sensitive point.
17. Normal hearing cats show shortest latencies in infragranular and granular layers [A. Mitani *et al.*, *J. Comp. Neurol.* **235**, 430 (1985); L. Aitkin, Ed., *The Auditory Cortex* (Chapman & Hall, London, 1990); J. J. Prieto, B. A. Peterson, J. A. Winer, *J. Comp. Neurol.* **344**, 349 (1994)]. These responses are found in a time window of 7 to 9 ms. Thereafter, massive activation of the supragranular layers occurs only shortly delayed in comparison with the activity in granular layers. This most likely reflects direct activation of these layers from layer IV. Long-lasting activation of infragranular layers is seen next, corresponding well with the functional anatomy of normal auditory cortex. There was almost no activation of infragranular layers in naïve deaf cats. The CSD signals were significantly lower than in normal controls (highest mean sink amplitude = 1117 μV/mm² in comparison with 1385 μV/mm²; one-tailed Wilcoxon–Mann-Whitney test, $P < 0.05$). After long-term electrical stimulation, in chronic animals, a pattern similar to normal hearing acutely deafened cats was observed. Sink amplitudes were significantly higher than in naïve CDCs (highest mean value = 1805 μV/mm²); they were also 30% higher than those of normal controls, but the difference between chronically stimulated deaf and normal cats was nonsignificant.
18. R. L. Snyder, S. J. Rebscher, K. Cao, P. A. Leake, K. Kelly, *Hear. Res.* **50**, 7 (1990); R. L. Snyder, S. J. Rebscher, P. A. Leake, K. Kelly, K. Cao, *ibid.* **56**, 246 (1991).
19. N. Hardie and R. K. Shepherd, *ibid.* **128**, 147 (1999).
20. P. A. Leake and G. T. Hradek, *ibid.* **33**, 11 (1988); ———, S. J. Rebscher, R. L. Synder, *ibid.* **54**, 251 (1991).
21. N. Wurth, S. Heid, A. Kral, R. Klinke, *Göttingen Neurobiol. Rep.* **27**, 318 (1999).
22. N. Kraus *et al.*, *Hear. Res.* **65**, 118 (1993).
23. R. Rajan and D. R. F. Irvine, *Audiol. Neurootol.* **3**, 123 (1998).
24. R. Hartmann, G. Topp, R. Klinke, *Hear. Res.* **13**, 47 (1984); C. van den Honert and P. H. Stypulkovski, *ibid.* **14**, 225 (1984).
25. J. S. Bakin and N. M. Weinberger, *Brain Res.* **536**, 271 (1990); M. P. Kilgard and M. M. Merzenich, *Science* **279**, 1714 (1998).
26. The authors thank M. Behrendt, N. Krimmel, M. Pramateftakis, C. Fritzsch, K.-F. Winter, and T. Wulf for important technical contributions; M. Kock for breeding the animals; N. Birbaumer and E. Friauf for their helpful comments on an earlier version of the manuscript; and the anonymous reviewers. Supported by the Deutsche Forschungsgemeinschaft (SFB 269).

30 April 1999; accepted 29 July 1999

A Chemical Inhibitor of p53 That Protects Mice from the Side Effects of Cancer Therapy

Pavel G. Komarov,[1,2]* Elena A. Komarova,[1]* Roman V. Kondratov,[1,5] Konstantin Christov-Tselkov,[3] John S. Coon,[2] Mikhail V. Chernov,[4] Andrei V. Gudkov,[1]†

Chemotherapy and radiation therapy for cancer often have severe side effects that limit their efficacy. Because these effects are in part determined by p53-mediated apoptosis, temporary suppression of p53 has been suggested as a therapeutic strategy to prevent damage of normal tissues during treatment of p53-deficient tumors. To test this possibility, a small molecule was isolated for its ability to reversibly block p53-dependent transcriptional activation and apoptosis. This compound, pifithrin-α, protected mice from the lethal genotoxic stress associated with anticancer treatment without promoting the formation of tumors. Thus, inhibitors of p53 may be useful drugs for reducing the side effects of cancer therapy and other types of stress associated with p53 induction.

p53 functions as a key component of a cellular emergency response mechanism. In response to a variety of stress signals, it induces growth arrest or apoptosis, thereby eliminating damaged and potentially dangerous cells from the organism (*1*). The *p53* gene is lost or mutated in most human tumors (*2*). Lack of functional p53 is accompanied by high rates of genomic instability, rapid tumor progression, resistance to anticancer therapy, and increased angiogenesis (*3*). p53 deficiency in mice is associated with a high frequency of spontaneous cancers (*4*). On the basis of all these observations, the inactivation of p53 is viewed as an unfavorable event, and much effort has been expended to facilitate anticancer treatment by restoring p53 function.

However, the role of p53 in cancer treatment is not limited to its involvement in killing tumor cells. In mice, the *p53* gene is highly expressed in several normal tissues, including lymphoid and hematopoietic organs, intestinal epithelia, and the testis, and it is these tissues that are damaged by anticancer therapy (*5*, *6*). p53-dependent apoptosis occurs in sensitive tissues shortly after gamma irradiation (*6*, *7*), and p53-deficient mice survive higher doses of gamma irradiation than do wild-type animals (*8*). These data indicate that p53 is a determinant of the toxic side effects of anticancer treatment, and thus may be an appropriate target for therapeutic suppression to reduce the damage to normal

[1]Department of Molecular Genetics, University of Illinois at Chicago, Chicago, IL 60607, USA. [2]Department of Pathology, Rush Presbyterian St. Luke's Medical Center, Chicago, IL 60612, USA. [3]Department of Surgical Oncology, University of Illinois at Chicago, Chicago, IL 60612, USA. [4]Research Institute, Cleveland Clinic Foundation, Cleveland, OH 44195, USA. [5]Quark Biotech, Pleasanton, CA 94566, USA.

*These authors contributed equally to this work.
†To whom correspondence should be addressed. E-mail: gudkov@uic.edu

tissues (*9*). This approach would be applicable only for tumors that lack functional p53.

To explore the feasibility of this approach, we isolated a chemical inhibitor of p53 and characterized its effects in vitro and in vivo. As a primary read-out system for screening of p53 inhibitors, we used the mouse ConA cell line, which carries the wild-type *p53* gene and the bacterial *lacZ* reporter gene under the control of a p53-responsive promoter (*6*). Because the inhibitors of p53 transactivation may not necessarily suppress apoptosis, the selected compounds were then tested in mouse cell line C8, a conventional model of p53-dependent apoptosis (*10*). Individual compounds from a diverse collection of 10,000 synthetic chemicals (from DIVERSet, Chembridge Corporation, San Diego, California), in combination with the potent p53 inducer, doxorubicin (Dox), were added to ConA cells growing in 96-well plates, and activation of *lacZ*-encoded β-galactosidase (β-Gal) was determined by routine X-Gal staining after 24 hours of treatment (Fig. 1A). We chose compounds that attenuated β-Gal induction in Dox-treated cells with no effect on cell growth or survival rate and picked one of them for a detailed characterization. This synthetic, water-soluble, and stable compound, with a molecular weight of 367, blocked activation of p53-responsive *lacZ* in ConA cells induced not only by Dox but also by ultraviolet (UV) light (Fig. 1, B and C) and gamma radiation (*10*) in a dose-dependent manner. This compound also reduced activation of endogenous cellular p53-responsive genes, including *cyclin G*, *p21/waf1/cip1*, and *mdm2*, as judged by Northern (RNA) blot hybridization (Fig. 1D). We named it pifithrin-α (PFTα, an abbreviation for "p–fifty three inhibitor") (Fig. 1E).

To analyze the effect of PFTα on p53-mediated apoptosis, we used mouse embryo fibroblasts transformed with *E1a+ras*, line C8, which undergo rapid p53-dependent apoptosis in response to a variety of treatments (*11*). A 10 μM concentration of PFTα inhibited apoptotic death of C8 cells induced by Dox, etoposide, Taxol, cytosine arabinoside (Fig. 2A), UV light, and gamma radiation (*10*). The anti-apoptotic activity of PFTα was

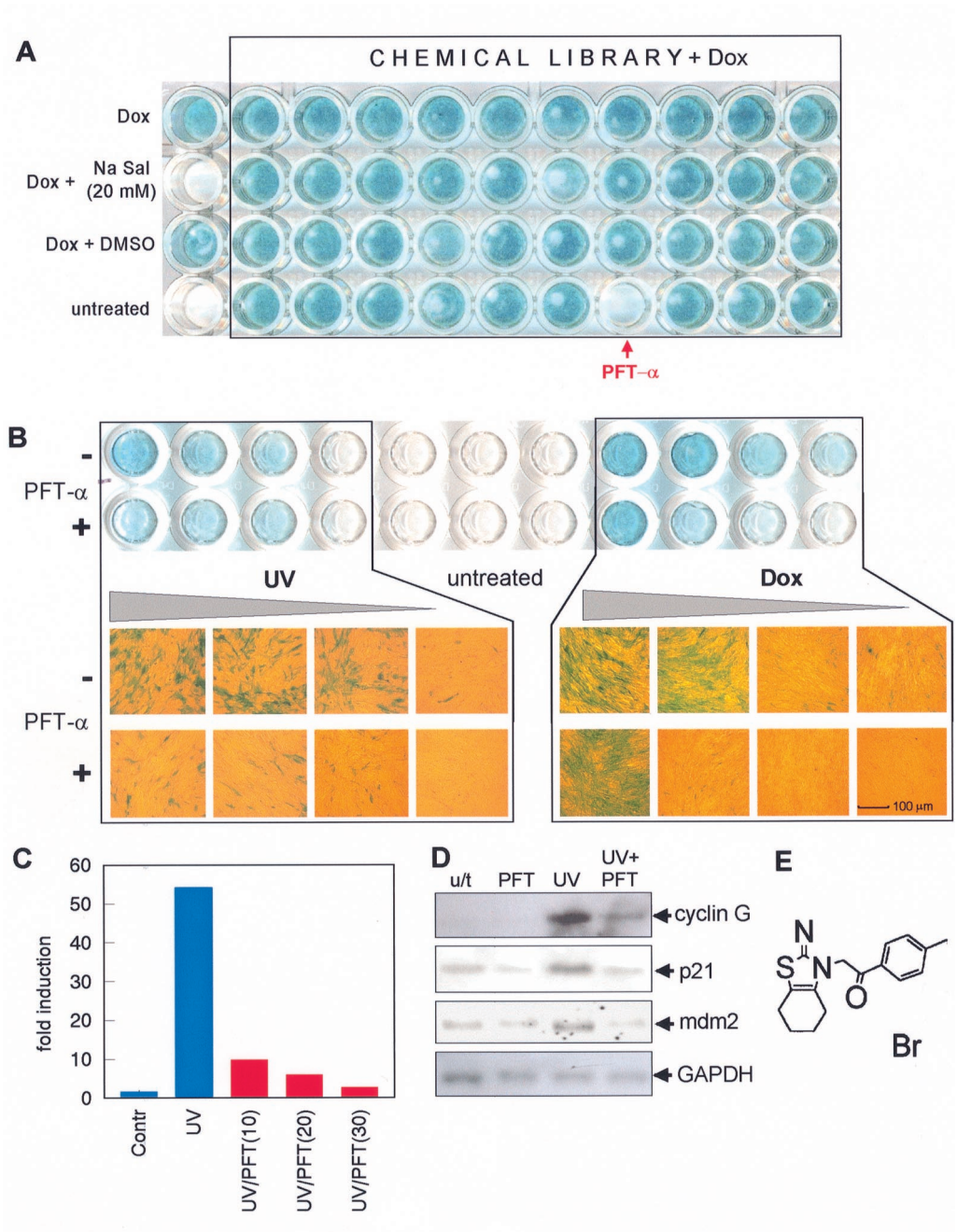

Fig. 1. Identification of a compound, PFTα, that inhibits p53-dependent transactivation of p53-responsive genes. (**A**) Screening of a chemical library (Chembridge) in ConA cells carrying the *lacZ* reporter gene under the control of a p53-responsive promoter. *lacZ*-encoded β-Gal was detected by X-Gal staining. ConA cells plated in 96-well plates were treated for 14 hours with Dox (0.2 μg/ml) in the presence of compounds at concentrations of 10 to 20 μM. The well containing PFTα is indicated by a red arrow. Control wells (left column) contained untreated ConA cells, treated with Dox alone or with Dox plus 20 mM sodium salicilate (Na Sal), which inhibits p53 transactivation (*19*). DMSO, dimethyl sulfoxide. (**B**) PFTα inhibits activation of *lacZ* in ConA cells treated with different dosages of UV (35, 25, 15, and 7 J/m^2) or Dox (for 10 hours at concentrations of 0.1, 0.2, 0.4, and 0.6 μg/ml). A fragment of a 96-well plate and regions of cell monolayers are shown. (**C**) Dependence of β-Gal activity in UV-irradiated (25 J/m^2) ConA cells on the concentration of PFTα (10, 20, and 30 μM). Cells were collected 8 hours after UV treatment, and β-Gal expression in the extracts was estimated by a colorimetric assay (*7*). (**D**) PFTα inhibits UV-induced transactivation of *cyclin G*, *p21/waf1*, and *mdm2*, which are known p53-responsive genes (*20*). Northern blots of RNA from ConA cells: u/t, untreated; PFT, incubated for 8 hours with 10 mM of PFTα; UV, 8 hours after UV treatment (25 J/m^2). (**E**) Chemical structure of PFTα [2-(2-imino-4,5,6,7-tetrahydrobenzothiazol-3-yl)-1-*p*-tolylethanone].

p53-dependent because it had no effect on the survival of UV-treated C8-56 cells, in which p53 is suppressed by a dominant negative mutant, GSE56 (*12*) (Fig. 2B), or of *E1a*+*ras*-transformed fibroblasts from $p53^{-/-}$ mouse embryos, line A4 (*10*, *11*). Similarly, PFTα inhibited p53-dependent growth arrest of human diploid fibroblasts in response to DNA damage but had no effect on p53-deficient fibroblasts. Suppression of both p53-dependent apoptosis and growth arrest by PFTα correlated with an increase in long-term cell survival, as judged by the results of assays of colony growth (*13*).

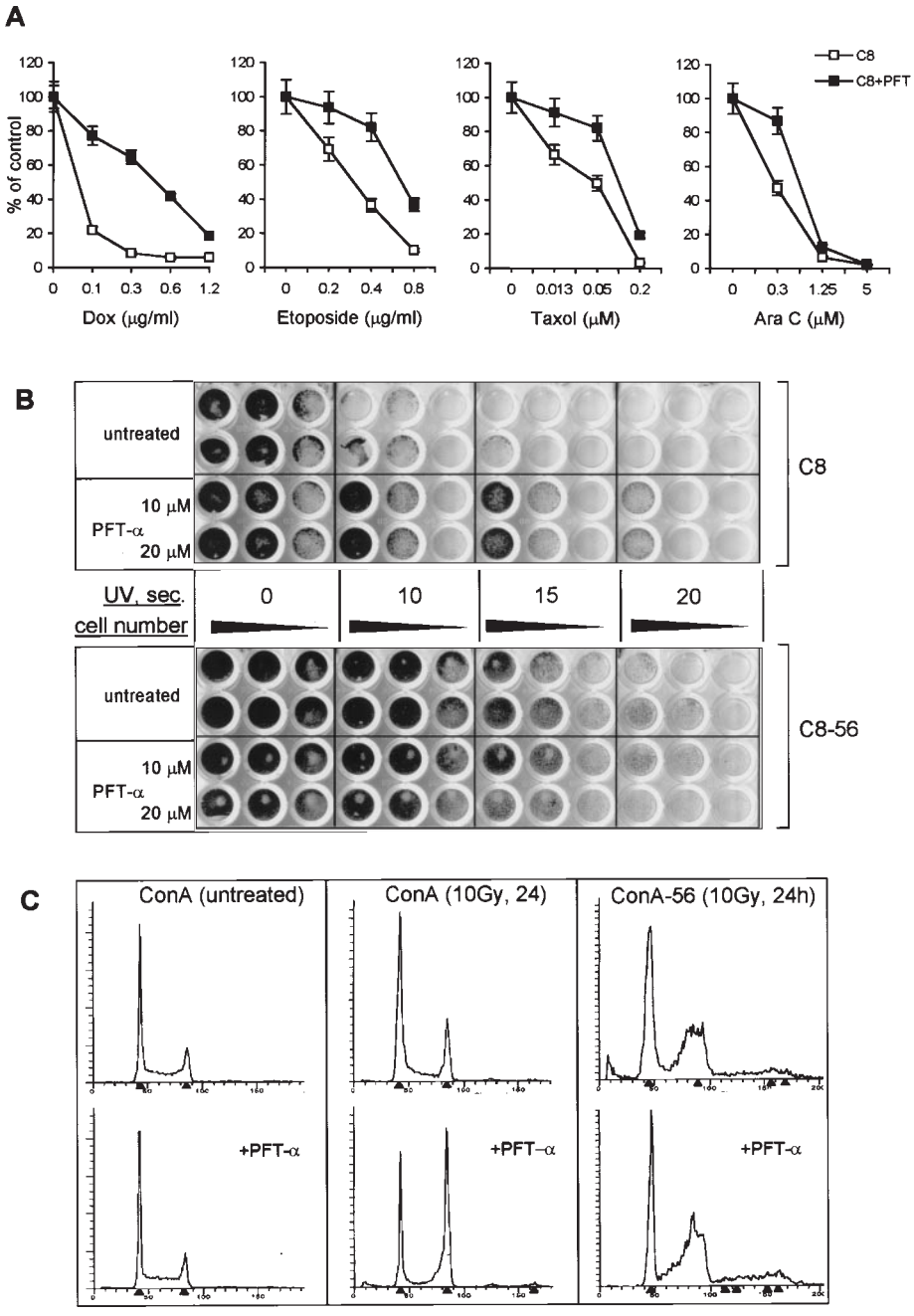

Fig. 2. PFTα modulates cellular functions of p53. (**A**) A 10 μM concentration of PFTα inhibits apoptosis in C8 cells treated with various cytotoxic compounds. C8 cells were treated 48 hours with the indicated concentrations of drugs, with and without PFTα. At the end of treatment, the number of attached cells was estimated by staining with 0.25% crystal violet in 50% methanol, followed by elution of the dye with 1% SDS. Optical density (530 nm) reflecting the number of stained cells was determined with a Bio-Tek EL311 microplate reader. (**B**) Inhibition of apoptosis by PFTα is p53-dependent (comparison of two cell lines differing in p53 status). Addition of PFTα (10 and 20 μM, as indicated) inhibits apoptosis of C8 cells but has no effect on the UV sensitivity of C8-56 cells, which express the dominant negative p53 mutant GSE-56 (*12*). Cells were plated at three different densities in 96-well plates and were treated with different doses of UV (indicated in seconds of illumination) with or without 10 or 20 μM concentrations of PFTα. Plates were fixed 48 hours after treatment and stained with crystal violet. (**C**) PFTα changes the cell cycle distribution of ConA cells 24 hours after gamma irradiation (10 Gy) but does not affect ConA cells expressing the dominant negative mutant of p53 GSE56 (ConA-56).

To test whether PFTα affects p53-dependent cell cycle checkpoint control, we compared the cell cycle distribution of treated ConA cells before and after gamma irradiation (Fig. 2C). PFTα had no effect on non-irradiated cells, but it dramatically increased the proportion of G_2-arrested cells 24 hours after gamma irradiation. This effect was p53-dependent because it was completely abrogated in the GSE56 cells, which have no functional p53 (Fig. 2C).

To determine the stage in the p53 pathway that is targeted by PFTα, we analyzed the compound's effects when apoptosis was induced by direct overexpression of wild-type p53 with no genotoxic stress applied. PFTα dramatically inhibited killing of p53-deficient human sarcoma Saos-2 cells that in control cells occurred within 48 hours after transient transfection with p53-expressing plasmids (Fig. 3A). This suggests that PFTα acts downstream of p53. PFTα did not alter phosphorylation or sequence-specific DNA binding of p53 in ConA cells after DNA-damaging treatments, as judged by protein immunoblotting in combination with two-dimensional protein analysis and gel shift assays (Fig. 3, B through E). However, it slightly lowered the levels of nuclear, but not cytoplasmic, p53 induced by UV irradiation. In contrast, PFTα did not affect the nuclear-cytoplasmic ratio of the p53-inducible $p21^{waf1}$ protein (Fig. 3D). These observations suggest that PFTα may modulate the nuclear import or export (or both) of p53 or may decrease the stability of nuclear p53. Whether this is the only mechanism of PFTα action remains unclear.

We also characterized the dependence of cell survival after genotoxic stress on the time and duration of PFTα application (*13*). PFTα had almost no protective effect if it was added before (up to 18 hours) and removed immediately before UV treatment of C8 cells. However, a short 3-hour incubation with PFTα after UV treatment had a pronounced protective effect, whereas a 24-hour incubation provided maximal protection. PFTα did not rescue UV-irradiated cells from apoptosis if it was added 3 hours after UV irradiation. These observations indicate that although PFTα can efficiently inhibit p53-dependent apoptosis, its effects are reversible and require the presence of the drug. Because many cells survived a lethal dose of UV irradiation after only 3 hours of incubation with PFTα, we conclude that the UV-induced apoptotic death signal is significantly reduced within several hours and completely disappears within 24 hours of irradiation.

To analyze the in vivo effects of PFTα,

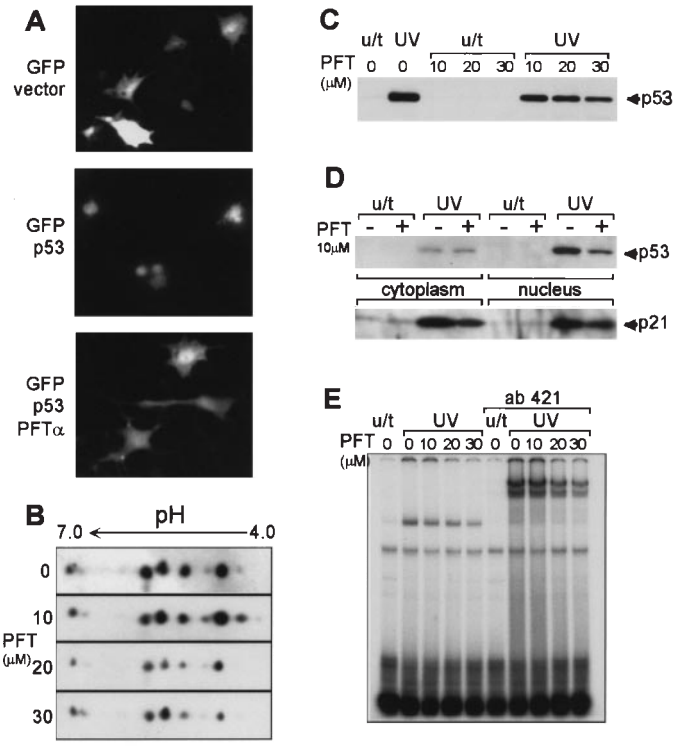

Fig. 3. Effects of PFTα on the p53 pathway. (**A**) PFTα inhibits apoptosis in Saos-2 cells transiently expressing p53. Cells were transfected with the plasmid DNA expressing green fluorescent protein (GFP) with the 5× excess of the plasmid carrying either wild-type human p53 (middle and bottom) or with no insert (top). Transfected cells were maintained with (bottom) or without (top and middle) PFTα. The majority of fluorescent cells transfected with p53-expressing plasmid undergo apoptosis 48 hours after transfection (middle). Apoptosis was inhibited in the presence of PFTα (bottom). (**B**) Comparison of spectra of p53 protein variants in the lysates of UV-irradiated (25 J/m^2) ConA cells in the presence of different concentrations of PFTα (0, 10, 20, and 30 μM) using two-dimensional protein gel electrophoresis. (**C**) PFTα partially and in a dose-dependent manner inhibits p53 accumulation in ConA cells after UV treatment (results of protein immunoblotting). PFTα was added to the cells before UV treatment and total cell lysates were prepared 18 hours later. (**D**) PFTα changes the nuclear and cytoplasmic distribution of p53. Nuclear and cytoplasmic fractions were isolated from UV-treated ConA cells 6 hours after UV irradiation. p53 and p21^{waf1} proteins were detected by immunoblotting. The nuclear and cytoplasmic ratios of p53 but not p21^{waf1} are significantly decreased in the PFTα-treated cells. (**E**) PFTα does not affect DNA-binding activity of p53. Results of a gel shift assay using cell lysates from either untreated or UV-irradiated ConA cells grown in medium containing PFTα are shown. The right half of the gel shows a supershift of the p53-binding DNA fragment by monoclonal antibody Pab421. The decline in the amount of bound DNA is proportional to the overall decrease in p53 content in the presence of PFTα.

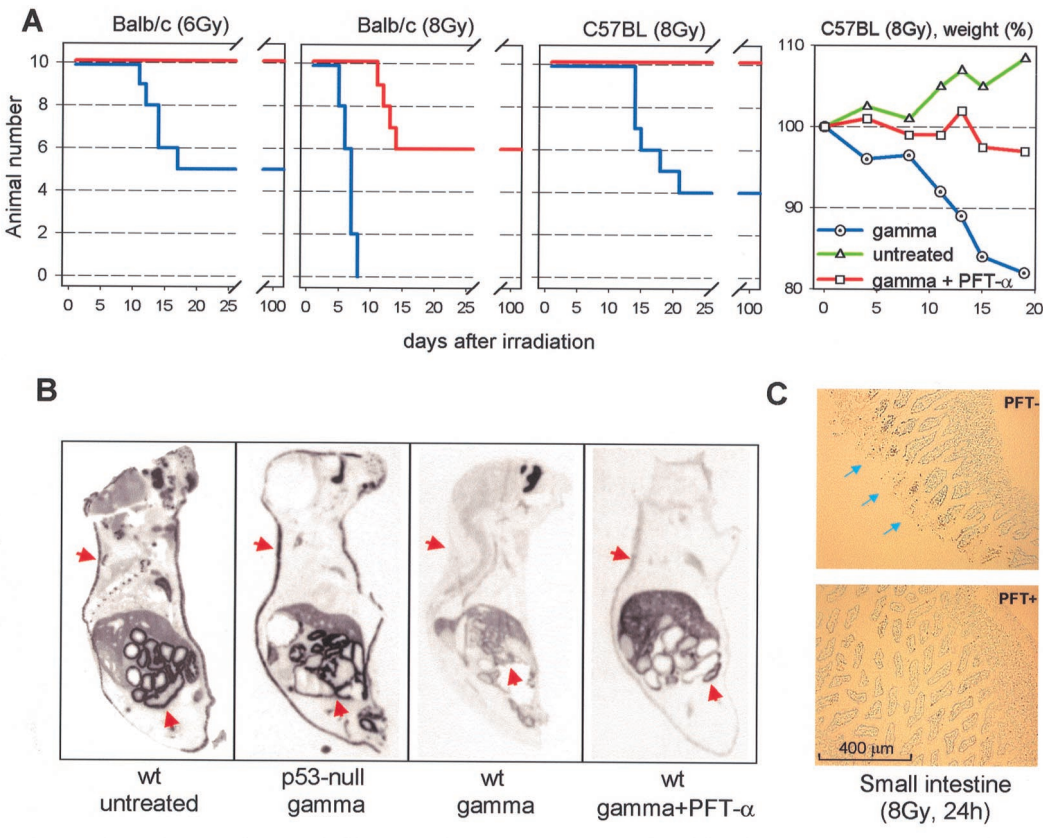

Fig. 4. Effects of PFTα in Balb/c and C57BL6 mice treated with whole-body gamma irradiation (results of representative experiments are shown). (**A**) A single i.p. injection of 2.2 mg per kilogram of body weight (mg/kg) of PFTα has a strong rescuing effect in both mouse strains. PFTα-injection abrogated the gradual loss of weight by C57BL6 mice after 8 Gy of gamma irradiation (the observed increase in the weight of the non-irradiated mice reflects the normal growth of young 5-week-old animals). The experiments were repeated at least three times with 10 mice per each experimental subgroup. Red traces indicate PFTα-treated animals; blue traces indicate PFTα-untreated animals. (**B**) PFTα abrogates p53-dependent regulation of DNA replication after genotoxic stress in vivo. ^{14}C-thymidine (10 mCi per animal) was injected intraperitoneally into untreated wild-type or p53-null mice and in gamma irradiated mice 8 hours after 10 Gy of whole-body gamma irradiation. A subgroup of the gamma-irradiated animals received one i.p. injection of PFTα (2.2 mg/kg) 5 min before irradiation. Mice were killed 24 hours after ^{14}C-thymidine injection, and whole-body sections (25 μm thick) were prepared and exposed with x-ray film in order to monitor the tissue distribution of ^{14}C. Red arrows indicate skin and intestine. (**C**) Comparison of tissue morphology and apoptosis (TUNEL staining) in the epithelium of the small intestine of C57BL6 p53 wild-type mice 24 hours after 10 Gy of whole-body gamma irradiation. Areas of massive apoptosis are indicated by blue arrows.

we treated two different strains of mice (C57BL and Balb/c) with lethal and sublethal doses of whole-body gamma radiation. We compared (i) untreated unirradiated mice, (ii) unirradiated mice that received a single intraperitoneal (i.p.) injection of PFTα, (iii) untreated gamma-irradiated mice, and (iv) mice injected intraperitoneally with PFTα immediately before gamma irradiation. PFTα treatment

completely rescued mice of both strains from 60% killing doses of gamma irradiation (8 Gy for C57BL and 6 Gy for Balb/c). Significant protection was also seen at higher doses of irradiation that were lethal for control animals (Fig. 4A). PFTα-injected mice lost less weight than irradiated mice that were not pretreated with the drug (Fig. 4B). PFTα did not protect p53-null mice from lethal irradiation, which confirms that it acts through a p53-dependent mechanism in vivo (*13*).

Drug-mediated suppression of p53 results in the survival of cells that otherwise would be eliminated by p53 and that may increase the risk of new cancer development. In fact, p53-deficient mice are extremely sensitive to radiation-induced tumorigenesis (*14*). However, in our study, no tumors or any other pathological lesions were found in the group of 30 survivors rescued from lethal gamma irradiation by PFTα, even at 7 months after irradiation. Thus, temporary suppression of p53 appears to differ from p53 deficiency in terms of cancer predisposition.

To monitor PFTα activity at the tissue level, we compared the effect of gamma radiation on DNA synthesis in tissues in PFTα-treated and untreated mice using a ^{14}C-thymidine incorporation assay. ^{14}C labeling of skin, gut, and several other tissues was significantly decreased after gamma irradiation in $p53^{+/+}$ mice but not $p53^{-/-}$ mice, reflecting the p53 dependence of the effect. The radiation-induced decrease in ^{14}C-thymidine incorporation was less pronounced in PFTα-treated mice than in control irradiated animals, presumably reflecting PFTα inhibition of p53 (Fig. 4B). These results suggest that PFTα attenuates the p53-dependent block of DNA replication in rapidly proliferating tissues after whole-body gamma irradiation. Changes in thymidine incorporation correlated with the extent of apoptosis in the gut epithelium of gamma-irradiated mice. The extensive apoptosis observed in the crypts and villi of the small intestine was abrogated in mice treated with PFTα before irradiation (Fig. 4C).

Our results raise the possibility of using PFTα (or other compounds with similar activity) to reduce the side effects of radiation therapy or chemotherapy for human cancers that have lost functional p53. Because the effects of PFTα are p53-dependent, the compound should not affect the sensitivity of such tumors to treatment. In fact, i.p. injection of PFTα did not change the radiation response of p53-deficient tumor xenografts in $p53^{+/+}$ nude mice (*15*).

It is likely that suppression of p53-dependent apoptosis has already been successfully and broadly applied to cancer patients in the form of growth factors supplementing chemotherapy (*16*). The therapeutic effect of such supplements may be associated with their activity as survival factors suppressing p53-dependent apoptosis (*17*). PFTα can now be used to determine whether there are any other clinical situations in which p53 suppression might be desirable. These include heart and brain ischemia, which both result from local hypoxia, a potent activator of p53 (*18*). Systematic screening of synthetic and natural compounds may lead to the identification of additional p53 inhibitors that may protect tissue from the consequences of a variety of stresses.

References and Notes

1. T. M. Gottlieb and M. Oren, *Biochim. Biophys. Acta* **1287**, 77 (1996).
2. A. J. Levine *et al.*, *Br. J. Cancer* **69**, 409 (1994); R. J. Steele, A. M. Thompson, P. A. Hall, D. P. Lane, *Br. J. Surg.* **85**, 1460 (1998).
3. C. Cordon-Cardo, J. Sheinfeld, G. Dalbagni, *Semin. Surg. Oncol.* **13**, 319 (1997); S. W. Lowe *et al.*, *Science* **266**, 807 (1994); G. J. Deichman *et al.*, *Int. J. Cancer* **75**, 277 (1998); K. M. Dameron, O. V. Volpert, M. A. Tainsky, N. Bouck, *Science* **265**, 1582 (1994).
4. L. A. Donehower *et al.*, *Nature* **356**, 215 (1992); T. Jacks *et al.*, *Curr. Biol.* **4**, 1 (1994).
5. A. Rogel, M. Popliker, C. G. Webb, M. Oren, *Mol. Cell. Biol.* **5**, 2851 (1985); P. Schmidt, A. Lorenz, H. Hameister, M. Montenarh, *Development* **113**, 857 (1991); D. Schwartz, N. Goldfinger, V. Rotter, *Oncogene* **8**, 1487 (1993).
6. E. A. Komarova *et al.*, *EMBO J.* **16**, 1391 (1997).
7. J. H. Hendry, A. Adeeko, C. S. Potten, I. D. Morris, *Int. J. Radiat. Biol.* **70**, 677 (1996); M. Hasegawa, Y. Zhang, H. Niibe, N. H. Terry, M. L. Meistrich, *Radiat. Res.* **149**, 263 (1998); J. H. Hendry, W. B. Cai, S. A. Roberts, C. S. Potten, *ibid.* **148**, 254 (1997); V. A. Tron *et al.*, *Am. J. Pathol.* **153**, 579 (1998).
8. C. H. Westfal *et al.*, *Cancer Res.* **58**, 5637 (1998); C. H. Westfal *et al.*, *Nature Genet.* **16**, 397 (1997).
9. E. A. Komarova and A. V. Gudkov, *Semin. Cancer Biol.* **8**, 389 (1998).
10. P. G. Komarov *et al.*, data not shown. All the conclusions and observations obtained with UV have been confirmed with gamma irradiation and adriamycin to verify the generality of the observed phenomena.
11. S. W. Lowe, H. E. Ruley, T. Jacks, D. Housman, *Cell* **74**, 957 (1993).
12. V. S. Ossovskaya *et al.*, *Proc. Natl. Acad. Sci. U.S.A.* **93**, 10309 (1996).
13. Supplemental information is available at *Science* Online at www.sciencemag.org/feature/data/1041963.shl.
14. C. J. Kemp, T. Wheldon, A. Balmain, *Nature Genet.* **8**, 66 (1994).
15. E. A. Komarova and A. V. Gudkov, unpublished data. The effect of PFTα on tumor response to radiation was tested in nude mice bearing tumors formed by $p53^{-/-}$ *E1a*+*ras*-transformed MEF cells (line A4). In preliminary experiments, PFTα injection, which protected mice from radiation-induced killing, did not affect the dynamics of tumor regression and regrowth in irradiated animals.
16. E. M. Johnston and J. Crawford, *Semin. Oncol.* **25**, 552 (1998).
17. M. Bronchud, *Anticancer Drugs* 4, 127 (1993).
18. T. G. Graeber *et al.*, *Nature* **379**, 88 (1996).
19. M. V. Chernov and G. R. Stark, *Oncogene* **14**, 2503 (1997); M. V. Chernov, C. V. Ramana, V. V. Adler, G. R. Stark, *Proc. Natl. Acad. Sci. U.S.A.* **95**, 2284 (1998).
20. K. Okamoto and D. Beach, *EMBO J.* **13**, 4816 (1994); W. S. El-Deiry *et al.*, *Cell* **75**, 817 (1993); X. Wu, J. H. Bayle, D. Olson, A. J. Levine *Genes Dev.* **7**, 1126 (1993).

21. We thank A. Polinsky for his generous help and R. Davidson for helpful comments on the manuscript. Supported in part by grants from NIH (CA75179 and CA60730) and Quark Biotech.

20 May 1999; accepted 10 August 1999

A Role for the Proteasome in the Light Response of the Timeless Clock Protein

Nirinjini Naidoo, Wei Song, Melissa Hunter-Ensor,* Amita Sehgal†

The cyclic expression of the period (PER) and timeless (TIM) proteins is critical for the molecular circadian feedback loop in *Drosophila*. The entrainment by light of the circadian clock is mediated by a reduction in TIM levels. To elucidate the mechanism of this process, the sensitivity of TIM regulation by light was tested in an in vitro assay with inhibitors of candidate proteolytic pathways. The data suggested that TIM is degraded through a ubiquitin-proteasome mechanism. In addition, in cultures from third-instar larvae, TIM degradation was blocked specifically by inhibitors of proteasome activity. Degradation appeared to be preceded by tyrosine phosphorylation. Finally, TIM was ubiquitinated in response to light in cultured cells.

In organisms ranging from cyanobacteria to mammals, the endogenous circadian clock is a feedback loop composed of cycling gene products that control their own synthesis. Such autoregulation has been demonstrated for the *period* (*per*) and *timeless* (*tim*) genes in *Drosophila melanogaster*, the *frequency* (*frq*) gene in *Neurospora*, the *kai* gene cluster in cyanobacteria, and appears to be true of the mammalian *per* genes (*1*, *2*). In all cases, precisely timed negative feedback by the proteins results in rhythmic expression of the RNA.

Rhythmic feedback is effected largely

Howard Hughes Medical Institute, Department of Neuroscience, University of Pennsylvania School of Medicine, Philadelphia, PA 19104, USA.

*Present address: Department of Biology, Massachusetts Institute of Technology, Cambridge, MA 02139, USA.

†To whom correspondence should be addressed. E-mail: amita@mail.med.upenn.edu